In Situ Investigation of Molecular Adsorption on Au Surface by Surface-Enhanced Infrared Absorption Spectroscopy

Toyoko Imae*,†,‡ and Hiroyuki Torii‡

Research Center for Materials Science and Graduate School of Science, Nagoya University, Nagoya 464-8602, Japan

Received: April 26, 2000; In Final Form: June 29, 2000

The kinetics of the self-assembled monolayer (SAM) formation of 3-mercaptopropionic acid (MPA) on Au surface and of the adsorption of hexadecyltrimethylammonium chloride (C_{16}TAC) on the SAM was investigated by surface-enhanced infrared absorption spectroscopy (SEIRAS) of attenuated total reflection (ATR) mode. The SAM formation of MPA depended on solvents. At the first stage of MPA adsorption in a chloroform-*d* solution, hydrogen-bonded MPA coexisted with free (non-hydrogen-bonded) MPA which was partly protonated. During the process of the adsorption, the free nonprotonated MPA was protonated or hydrogen-bonded. After the abundant SAM formation, alkyl backbone was rearranged. With adsorption in an ethanol solution, the hydrogen-bonded MPA SAM increased in content without any structural rearrangement. No free species and no protonated species were observed. The molecular orientation was also different between SAMs in chloroform-*d* and in ethanol. The dependence of the CH_2 antisymmetric stretching vibration band intensity on adsorption time was examined on the basis of the adsorption kinetics. It was confirmed that the MPA SAM formation on Au surface proceeds according to the simple Langmuir (monolayer) adsorption theory. On the other hand, the adsorption of C_{16}TAC on the MPA SAM obeyed the kinetics where the fast adsorption at an early stage is followed by the slow adsorption. ATR-SEIRAS indicated that there are the adsorption of C_{16}TAC on the MPA SAM and the transition of carboxylic acid to carboxylate. Finally, ion pairs connected by the electrostatic interaction are formed.

Introduction

Adsorption and desorption kinetics of molecules on solid substrates are important concerns in many applications such as colloidal stabilization, mineral flotation, lubrication, surface reaction, chemical separation, and so on. Such kinetics have experimentally and theoretically been explored.[1−5] Among films where molecules adsorb spontaneously onto the metal surfaces, one of the typical thin films with highly ordered array is a self-assembled monolayer (SAM). The SAM is expected to have many applications such as a molecular device, a microreaction matrix, and others. Since the efficiency of the application depends on the quality of the SAM, effort must be devoted to preparing high-quality SAM, which is controlled by kinetics. Different techniques were utilized to elucidate in situ kinetics of the SAM formation such as a quartz crystal microbalance (QCM) monitor method,[6−9] surface plasmon resonance spectroscopy,[10] and atomic force microscopy.[11]

Surface-enhanced infrared absorption spectrum (SEIRAS) is one of the convenient tools to determine the adsorption and desorption kinetics, since the infrared absorption bands are enhanced by the surface plasmon resonance phenomenon and the sensitivity to a small amount of molecules adsorbed on gold surface is very high.[12−15] Especially, SEIRAS at attenuated total reflection (ATR) mode is valuable to the investigation of adsorption from a solution to the solid surface.[5] Another advantage to using SEIRAS is the surface selection rule. Vibration bands with transition moments perpendicular to the metal surface are enhanced by the electric field normal to the surface. On the contrary, ones parallel to the surface are diminished. Therefore, the orientation of molecules on the surface is determined.

In the present work, we report the kinetics of the SAM formation on the gold surface and of the adsorption of small molecules on the SAM by using ATR-SEIRAS. We choose 3-mercaptopropionic acid (MPA) as a SAM-forming molecule in order to minimize the overlap of CH_2 absorption bands of MPA on those of an adsorbate, hexadecyltrimethylammonium chloride (C_{16}TAC). Spectroscopic investigation has been reported for SAMs of long alkyl chain alkylthiols or their derivatives[16−19] but very few for short chain compounds except cysteamine[13] because of the weak band intensities. It is introduced in this paper that ATR-SEIRAS detects such weak bands with enough intensity. The interaction between MPA SAM and C_{16}TAC is also discussed.

Experimental Section

MPA ($HSCH_2CH_2COOH$, 99+%) was purchased from Aldrich Chemical Co. C_{16}TAC ($CH_3(CH_2)_{15}N(CH_3)_3Cl$) from Tokyo Kasei Kogyo Co., Ltd. was recrystallized from an ethanol−acetone mixture. Chloroform-*d*, ethanol, and D_2O are products of Wako Pure Chemical Industries, Ltd. Chloroform-*d* and ethanol solutions of MPA (2 mM) were prepared. C_{16}TAC was dissolved in D_2O to be a 3 mM (0.1 wt %) concentration.

Fourier transform infrared (FT-IR) spectra were recorded on a Bio-Rad FTS 575C FT-IR spectrometer equipped with a cryogenic mercury cadmium telluride (MCT) detector. Band

* Author to whom correspondence should be addressed at Research Center for Materials Science, Nagoya University, Chikusa, Nagoya 464-8602, Japan. Tel: +81-52-789-5911. Fax: +81-52-789-5912. E-mail: imae@chem2.chem.nagoya-u.ac.jp.

† Research Center for Materials Science, Nagoya University.

‡ Graduate School of Science, Nagoya University.

10.1021/jp001592a CCC: $19.00
Published on Web 09/13/2000

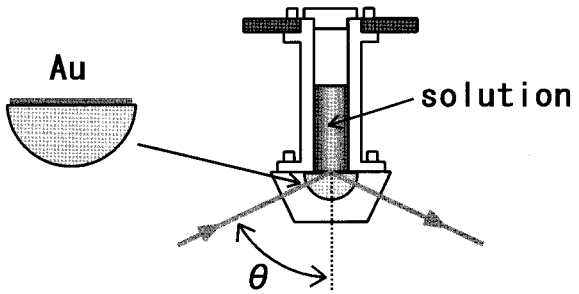

Figure 1. A schematic presentation of an ATR attachment for the SEIRAS measurement.

resolution was 4 cm^{-1}. All measurements were carried out at room temperature (~25 °C).

Transmission FT-IR spectra were measured for an aliquot of liquid MPA, which was pasted up on a CaF_2 window, and for a chloroform-*d* solution of MPA, which was filled in a solution cell with 0.025 mm path.

Infrared reflection absorption spectrum (IRAS) was taken using a Harrick reflectance attachment (Refractor) with a 75° incidence angle. The 200 nm gold film evaporated on a glass with a 150 nm chromium film was used as a substrate. The gold film substrates were cleaned by immersing them in a mixure of concentrated H_2SO_4 and aqueous H_2O_2 (30 v/v %) solution (3:1 in volume) for 10 min at ca. 80 °C. The substrates were kept for 2 h in an ethanol solution of MPA (2 mM) and rinsed by ethanol and ultrapure (Milli-Q) water, followed by drying. The obtained SAM was utilized for IRAS measurement.

ATR-SEIRAS was measured with an ATR attachment (See Figure 1). Gold was evaporated on a silicon prism at a rate of 0.05 As^{-1} under the pressure of ca. 3×10^{-4} Pa on a Shinku SD-240 vaporizing instrument (Shinku of Technology, Nagoya). The 10 nm gold island thickness was chosen as a condition to obtain the better surface-enhanced effect. A time-resolved ATR-SEIRAS measurement of MPA adsorption on the gold island film was started just after an ATR cell was filled by a chloroform-*d* or ethanol solution of MPA. After the equilibrium of MPA adsorption in ethanol was reached, the SAM film was rinsed by ethanol and used for ATR-SEIRAS measurement. An aqueous solution of C_{16}TAC was poured on the MPA SAM film, and a time-resolved ATR-SEIRAS was measured.

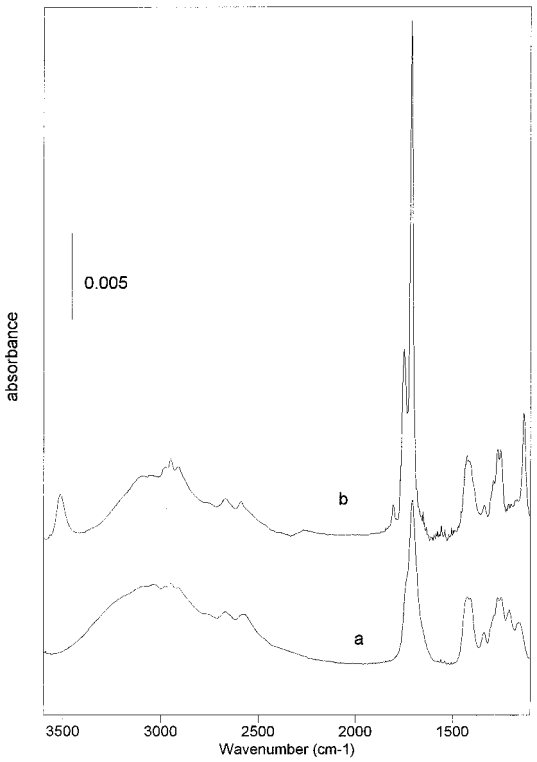

Figure 2. Transmission FT-IR spectra for an aliquot of liquid MPA (a) and for a chloroform-*d* solution of MPA (2 mM) (b). Background: (a) a CaF_2 window; (b) a 0.025 mm solution cell filled by chloroform-*d*. Accumulation: 16 times.

Results and Discussion

IR Spectrum of MPA. Figure 2 shows a transmission IR spectrum of liquid MPA. Band positions and their assignments are listed in Table 1. The assignments were performed,

TABLE 1: Observed IR Band Positions (cm^{-1})[a] and Their Assignments of MPA and C_{16}TAC

transmission IR		ATR-SEIRAS (time-resolved)		ATR-SEIRAS	IRAS	ATR-SEIRAS (time-resolved)	
liquid MPA	MPA in $CDCl_3$	MPA SAM in $CDCl_3$	MPA SAM in ethanol	MPA SAM from ethanol		C_{16}TAC in D_2O on MPA SAM	assignment[b]
	3518m	(3420b)[c]					free OH str
3100b	3100b	3165b					hydrogen-bonded OH str
3040b	3060b	3060b					hydrogen-bonded OH str
2984w	2984w	(2984s)[c]	2980s	2989m	2985m	2995vw	CH_2 antisym str
						2960vw	CH_3 asym str
2945w	2945w						
						2920w	CH_2 antisym str
2910w	2910w	(2902s)[c]	2902s	2900m	2902m		CH_2 sym str
						2850w	CH_2 sym str
2760sh	2760sh						overtone
2660m	2668w						overtone
2579m	2588w						SH str
	1752s						free C═O str
1711vs	1713vs	1710s	1705m	1710s	1730s	1677m	hydrogen-bonded C═O str
		1560m				1547m	COO^- antisym str
						1500w	CH_2 scissor
						1480w	CH_2 scissor
1414s	1414m	1414s[d])	1386m	1423s	1409vs	1389m[d]	C−O str coupled
1405s	sh		1371m	1400s	1380s	1370m[d]	with OH ip bend

[a] vs, very strong; s, strong; m, medium; w, weak; vw, very weak; b, broad; sh, shoulder. [b] str, stretching; antisym, antisymmetric; asym, asymmetric; sym, symmetric; scissor, scissoring; ip, in-plane; bend, bending; wag, wagging; twist, twisting. [c] The bands were observed in the transition period of PMA SAM formation. See the text. [d] The COO^- symmetric stretching vibration mode is overlapped.

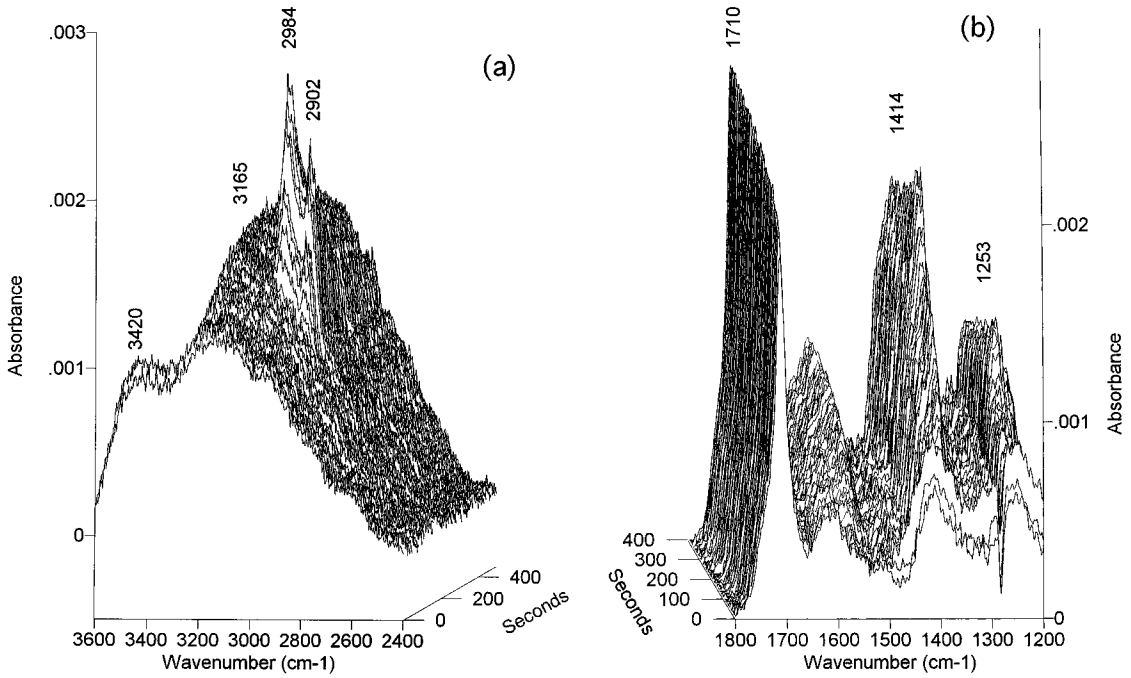

Figure 3. A time-resolved ATR-SEIRAS of MPA adsorption from a chloroform-*d* solution of MPA (2 mM). Background: an ATR cell filled by chloroform-*d* on gold island film. Measurement: 300 sets of 4 times accumulation. (a) 3600−2400 cm^{-1} region; (b) 1800−1200 cm^{-1} region.

according to the previous reports.[20,21] There are broad bands at ∼3100 cm^{-1} and a strong band at 1711 cm^{-1}, which are assigned to the OH and C═O stretching vibration bands, respectively. Lower wavenumbers of these bands suggest the hydrogen-bonding between carboxylic acid groups of MPAs.[22] Three bands at 2984, 2945, and 2910 cm^{-1} were observed in the CH_2 stretching vibration band region. Wavenumbers of these bands are so high that ethylene groups of MPA are not assigned to the trans-zigzag configuration. A 2579 cm^{-1} band is assigned to the SH stretching vibration mode.

An IR spectrum of a chloroform-*d* solution of MPA was compared with that of liquid MPA in Figure 2 and Table 1. The remarkable difference is the appearance of 3518 and 1752 cm^{-1} bands. These bands can be assigned to the free OH and C═O stretching vibration modes, indicating the coexistence of hydrogen-bonding-free MPA in chloroform-*d*.[23] The ratio 1:3 of free MPA:hydrogen-bonded MPA was obtained from their intensity ratio. The SH stretching vibration band (2588 cm^{-1}) in chloroform-*d* is higher than that of liquid state.

MPA SAM Formation in Chloroform-*d*. A time-resolved ATR-SEIRAS for MPA adsorption on gold island film in chloroform-*d* is shown in Figure 3. Even immediately after the adsorption started, the formation of SAM is confirmed from the absence of the SH stretching vibration band. Band positions and their assignments are listed in Table 1.

A remarkable difference of ATR-SEIRAS from the transmission IR spectrum in chloroform-*d*, besides the disappearance of the SH stretching vibration band, is the appearance of a 1560 cm^{-1} band which is assigned to the COO^- antisymmetric stretching vibration mode. The COO^- symmetric stretching vibration band must be overlapped on a 1414 cm^{-1} band of the C−O stretching vibration mode coupled with the OH in-plane bending vibration mode, since this band is intensified as well as the 1560 cm^{-1} band with adsorption time. This suggests that carboxylic acids of MPA are deprotonated during the SAM formation. The fraction of carboxylate against carboxylic acid is 0.2−0.3 and increases with the SAM formation.

A broad OH vibration band at ∼3420 cm^{-1} and a C═O stretching vibration band at 1752 cm^{-1} are weakened with time

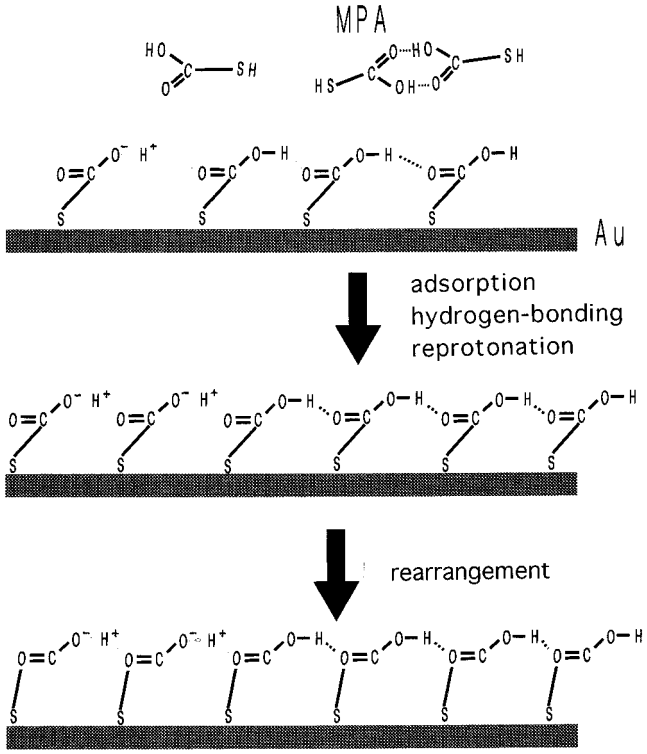

Figure 4. A schematic presentation of MPA adsorption from a chloroform-*d* solution on gold surface.

but bands at ∼3165 and ∼3060 cm^{-1} are intensified. This indicates that some of free carboxylic acid groups of MPA adsorbed on the gold film are deprotonated and some are hydrogen-bonded with time. The intensities of the CH_2 antisymmetric and symmetric vibration bands at 2984 and 2902 cm^{-1}, respectively, were increased with the SAM formation until ca. 200 s but were decreased after that, suggesting the rearrangement of ethylene configuration from tilt to normal direction against the gold surface after the hydrogen-bonding formation.

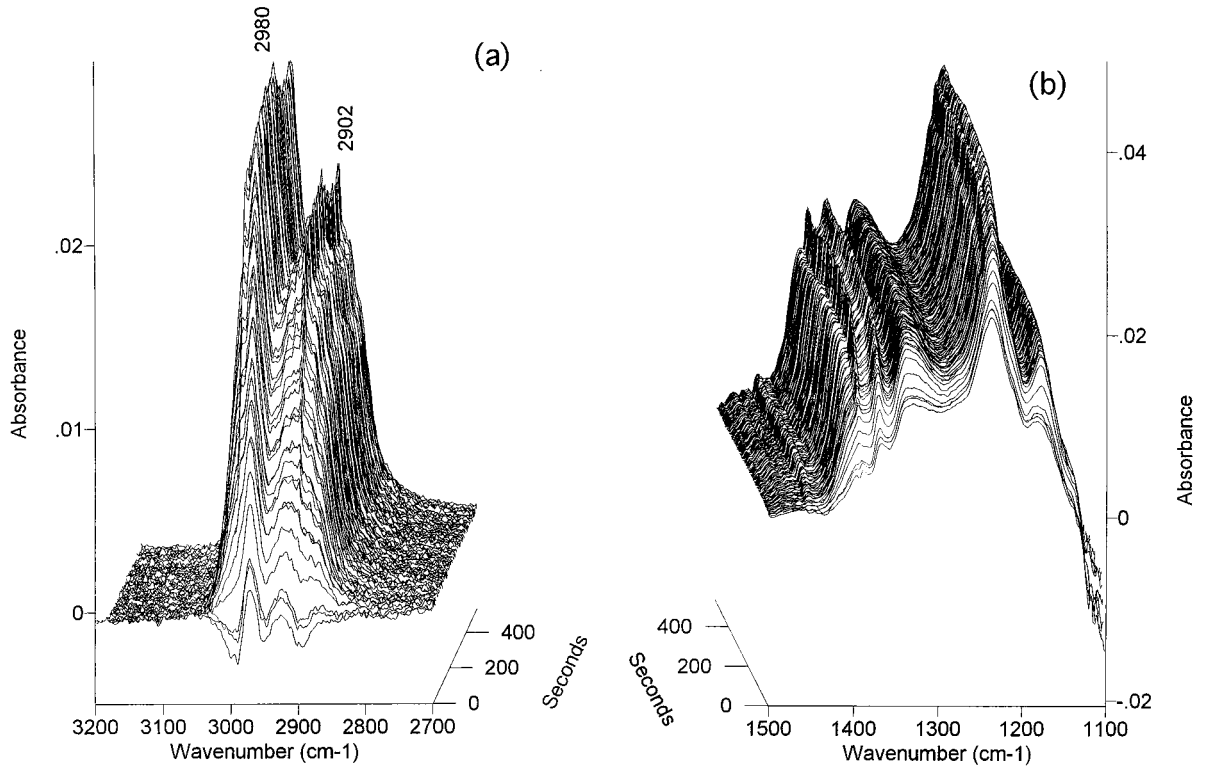

Figure 5. A time-resolved ATR-SEIRAS of MPA adsorption from an ethanol solution of MPA (2 mM). Background: an ATR cell filled by ethanol on gold island film. Measurement: 300 sets of 4 times accumulation. (a) 3200−2700 cm^{-1} region; (b) 1500−1100 cm^{-1} region.

Figure 4 illustrates the scheme of MPA adsorption on the gold surface in chloroform-*d*. During short adsorption time, many MPA molecules adsorb on the gold surface. At the first stage of adsorption, there coexist free and hydrogen-bonded MPAs, and free MPA is partly protonated. During the process of the adsorption, the free MPA is protonated or hydrogen-bonded. After an abundant amount of SAM was formed, the alkyl backbone is rearranged toward a more normal direction to the gold surface.

MPA SAM Formation in Ethanol. A time-resolved ATR-SEIRAS for MPA adsorption on the gold island film was measured even from an ethanol solution and is shown in Figure 5. Although the CH_2 stretching vibration bands at 2980 and 2902 cm^{-1} are increased with increasing adsorption time, the OH stretching vibration bands and the meaningful COO^- stretching vibration bands are not observed in ethanol, different from the MPA adsorption from a chloroform-*d* solution, as compared in Table 1.

Figure 6 shows an ATR-SEIRAS of MPA SAM which was prepared by removing the solution on gold island film in a ATR cell and rinsing by ethanol. IRAS of MPA SAM, which was prepared on the gold film from an ethanol solution, is compared in Figure 6. The IR spectra are similar to each other and to that in ethanol (see Figure 5 and Table 1), although the intensity of IRAS is 20 times weaker than that of ATR-SEIRAS, suggesting the efficiency of ATR-SEIRAS in the investigation of tiny amounts of adsorption.

When compared with a transmission IR spectrum of liquid MPA (Figure 2a), in contrast with the similarity of absorption bands in a region below 2000 cm^{-1}, bands at the region above 2500 cm^{-1} are different. Although the CH_2 antisymmetric and symmetric vibration bands are observed at 2989 and 2900 cm^{-1}, respectively, a SH stretching vibration band disappears, indicating the formation of SAM. The OH stretching vibration bands are also absent, and the intensity of the hydrogen-bonded C═O stretching vibration band (1710 cm^{-1}) is weakened in comparison with bands associated with the CH_2 group and others.

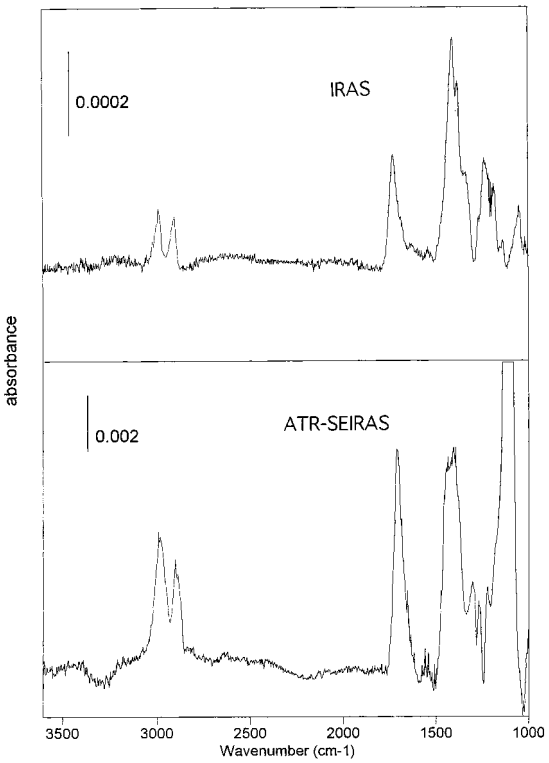

Figure 6. IRAS (upper) and ATR-SEIRAS (lower) for MPA SAM. Background: gold substrate. Accumulation: 256 times.

The adsorption mechanism is rather simple in ethanol in comparison with that in chloroform-*d*, as seen in Figure 7. With adsorption, the hydrogen-bonded MPA SAM is formed and only the content increases without any rearrangement in the molecular

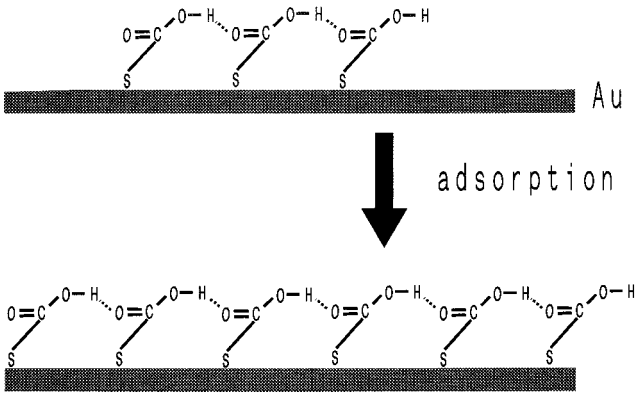

Figure 7. A schematic presentation of MPA adsorption from an ethanol solution on gold surface.

structure. There are no free species and no protonated species. The hydrogen-bonded OH axes must be located parallel to the gold surface, since the OH stretching vibration bands are not observed. The hydrogen-bonded C═O and alkyl backbone axes must be more parallel and tilt, respectively, to the Au surface, because the band intensity of the C═O stretching vibration mode is weak and the band intensity of the CH_2 stretching vibration mode is maintained. It may be noticed that, the adsorption mechanism in ethanol is different from in chloroform-*d*, although we cannot explain the reason for such difference in the present situation.

C_{16}TAC Adsorption on MPA SAM. Figure 8 shows a time-resolved ATR-SEIRAS of C_{16}TAC-adsorbed MPA SAM on Au island film. Band positions and their assignments are listed in Table 1. Although a very weak CH_2 stretching vibration band of MPA at 2995 cm^{-1} keeps its intensity, the bands of C_{16}TAC appearing at 2920 and 2850 cm^{-1} are intensified with time, indicating the time-dependent adsorption of C_{16}TAC. Frequencies of these bands are completely different from those of MPA but similar to those of long alkyl chains in trans-zigzag configuration,[24] suggesting highly ordered hydrocarbon chains.[22] It is seen that the CH_2 stretching vibration band intensities of the long alkyl chain in C_{16}TAC dominate those of ethylene in MPA, and the CH_3 stretching vibration band of C_{16}TAC is less remarkable than the CH_2 stretching vibration band. These results support that the alkyl chain of C_{16}TAC adsorbed on the MPA SAM must be tilted from the normal to the gold surface.

A band at 1677 cm^{-1} is assignable to the hydrogen-bonded C═O stretching vibration mode of MPA and shifted to the lower-frequency region in comparison with 1730 or 1713−1705 cm^{-1} in liquid MPA, MPA in chloroform-*d*, and MPA SAM without C_{16}TAC. The bands at similar positions were reported for Langmuir−Blodgett films of a cinnamic acid derivative by Yamamoto et al.[25] The 1730 cm^{-1} band was assigned to the "lateral hydrogen-bonded state" which was imaged linear hydrogen-bonded chains of carboxyl groups in the monolayer. The 1684 and 1674 cm^{-1} bands were to the "cis configuration of hydrogen-bonded dimers" and the 1715 cm^{-1} band was to the "face-to-face hydrogen-bonded state" between neighboring monolayers. Ozaki et al.[22] suggested that doublet bands at ∼1709 and 1963 cm^{-1} for the monolayer Langmuir−Blodgett film of arachidic acid are due to the coexistence of trans and cis configurations between the neighboring molecules or between the monolayer and substrate. Since their band positions and assignments are not necessarily fit to the present SAM, the more detail assignments for the hydrogen-bonded C═O stretching vibration bands of MPA are ambiguous for the moment.

The COO^- antisymmetric vibration band of MPA appears at 1547 cm^{-1} even immediately after the adsorption started. The intensity of the COO^- stretching vibration band is increased with adsorption time, and simultaneously the C═O stretching vibration band is diminished. This means the deprotonation of carboxylic acid of MPA during C_{16}TAC adsorption on the MPA SAM. The COO^- symmetric vibration band should be over-

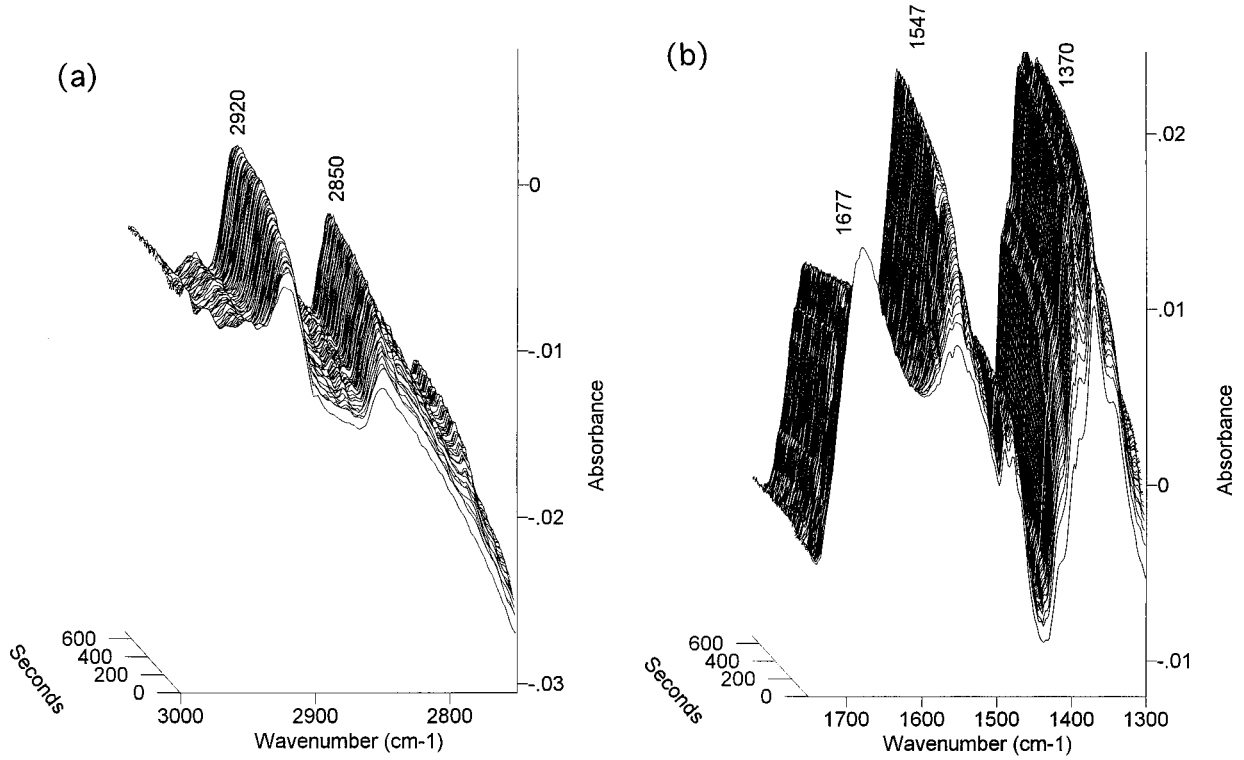

Figure 8. A time-resolved ATR-SEIRAS of C_{16}TAC adsorption from a D_2O solution of C_{16}TAC (3 mM) on MPA SAM. Background: gold island film. Measurement: 250 sets of 4 times accumulation. (a) 3000−2700 cm^{-1} region; (b) 1750−1300 cm^{-1} region.

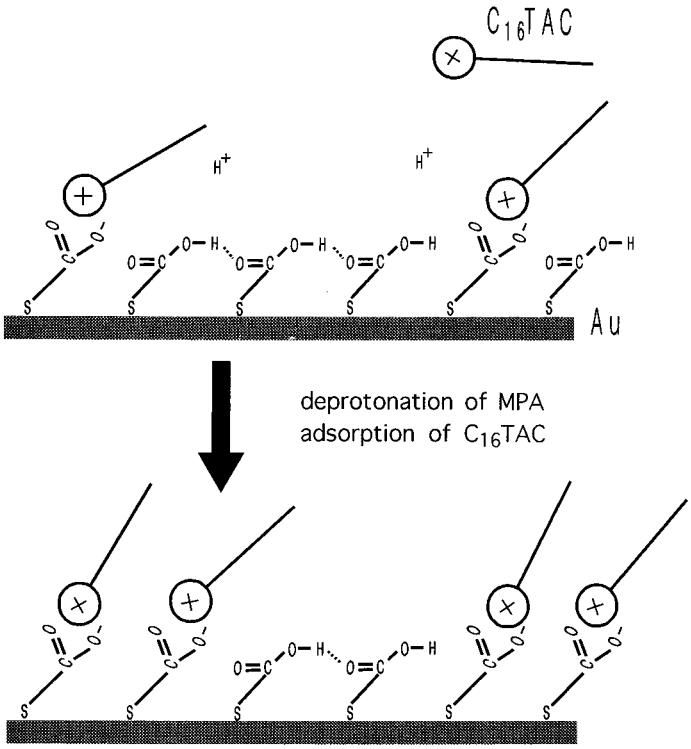

Figure 9. A schematic presentation of $C_{16}TAC$ adsorption from a D_2O solution on MPA SAM.

lapped on the C−O stretching vibration band coupled with the OH in-plane bending vibration mode at ~1380 cm^{-1}, because the doublet band is intensified as well as the COO^- antisymmetric vibration band.

The CH_2 scissoring vibration band of $C_{16}TAC$ arises at ~1500 cm^{-1}. The mode is split into a doublet, indicating the intermolecular interaction and thus the orthorhombic molecular packing of $C_{16}TAC$ in the adsorbed layer.[22,26] This is consistent with the feature obtained from the CH_2 stretching vibration bands.

As illustrated in Figure 9, the adsorption of $C_{16}TAC$ on MPA SAM should be due to the electrostatic interaction, since the carboxylic acid of MPA changes to carboxylate with the progress of adsorption. The adsorbed $C_{16}TAC$ has the trans-zigzag alkyl chain configuration but does not arrange with the normal direction to the gold surface, as estimated from the CH_2 and CH_3 stretching vibration bands.

Kinetics of MPA SAM Formation on Au Surface and of $C_{16}TAC$ Adsorption on MPA SAM. Some theoretical equations were proposed for adsorption and desorption kinetics. The basic theory is based on the Langmuir (monolayer) model where only adsorption and desorption are taken into account,[8,11] that is,

$$I(t) = I_\infty\{1 - \exp(-k_{app}t)\} \quad (1)$$

where $I(t)$ and I_∞ are the adsorption amounts at time t and infinite time, respectively. An apparent rate constant k_{app} ($= k_aC + k_d$) is a function of the intrinsic rate constants k_a and k_b for adsorption and desorption, respectively, and the bulk concentration of adsorbate C. The diffusion-limited first-order (DIF) Langmuir model,[10] where diffusion processes limit the rate of the adsorption process, must be considered at lower concentrations and described as

$$I(t) = I_\infty\{1 - \exp(-k_{app}t^{1/2})\} \quad (2)$$

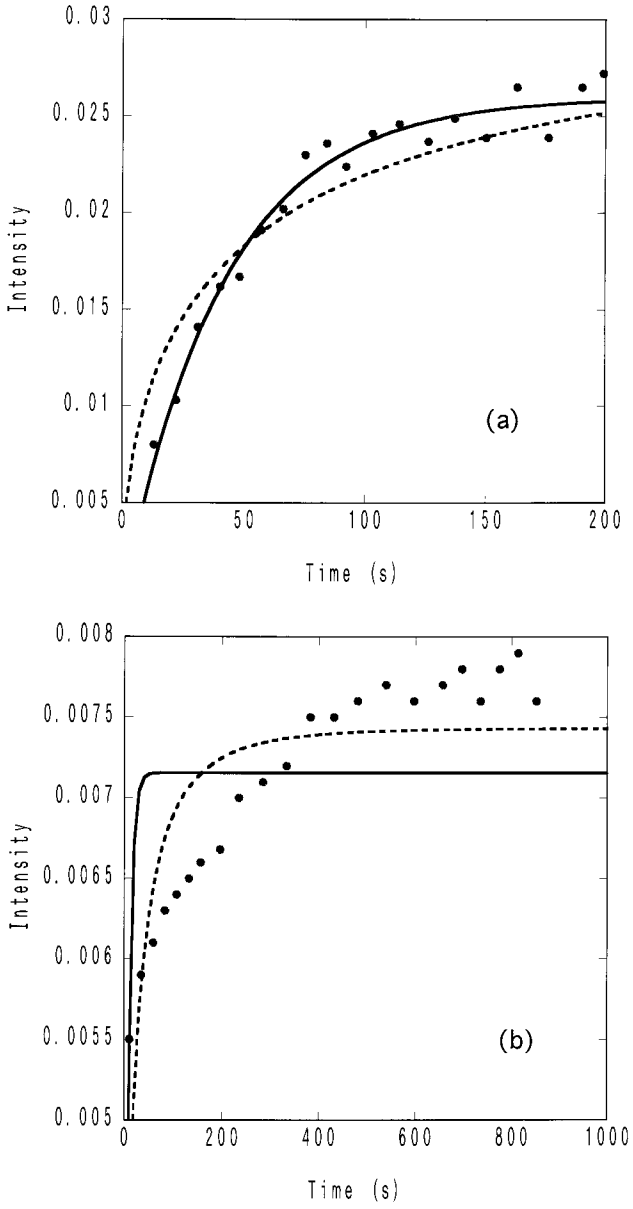

Figure 10. Intensity increase of a CH_2 antisymmetric stretching vibration band as a function of adsorption time. (a) MPA adsorption from an ethanol solution on gold film; (b) $C_{16}TAC$ adsorption from a D_2O solution on MPA SAM. ●, observed; —, Langmuir model; - - -, diffusion-limited first-order Langmuir model.

Other more complicated models such as a second-order non-diffusion-limited model[10] were also used.

Intensity increase of a CH_2 antisymmetric stretching vibration band as a function of adsorption time for MPA adsorption on gold surface in ethanol is plotted in Figure 10a and compared with curves calculated on the basis on Langmuir and DIF Langmuir models and the assumption of the linear relation of adsorption amount and IR band intensity. The Langmuir model presents a better fit to the observed values than the DIF Langmuir model. The apparent rate constant calculated was 0.024 s^{-1} for fitting to eq 1. The apparent rate constant of (3 or 7.5) × 10^{-4} s^{-1} for the formation of mercaptoundecanoate ($HSC_{10}H_{22}COO^-$) SAM on gold from an aqueous solution was obtained by the application of the Langmuir rate low for atomic force microscopic data.[11] The similar procedure for QCM data displayed a rate constant of (1.6−16) × 10^{-4} s^{-1} for an alkanethiol SAM on gold from an ethanol solution[6,8] and of 0.06−0.90 s^{-1} for a 1-octadecanethiol SAM on gold from

organic solvents.[7] The characteristic rate constant for the SAM formation of MPA is the same order as that for a 1-octadecanethiol SAM but much larger than the others. The reason for such a large difference is mysterious.

Williams et al.[27] have reported that the adsorption kinetics of unilamellar vesicles onto SAM dramatically depends on the composition of mixed SAM, although they elucidated only qualitatively the results. The quantitative analysis of the adsorption kinetics of C_{16}TAC on MPA SAM is shown in Figure 10b, where the intensity increase of a CH_2 antisymmetric stretching vibration band of C_{16}TAC as a function of adsorption time for the C_{16}TAC adsorption in water on the MPA SAM is compared with curves calculated on the basis of Langmuir and DIF Langmuir models and the assumption of the linear relation of adsorption amount and IR band intensity. It is apparent that both Langmuir and DIF Langmuir models do not match the observed values. The second-order non-diffusion-limited model is also not close enough to the observed data. The observation seems to be through the fast adsorption at the early stage followed by the slow adsorption. The two-step process of the adsorption was reported before.[8,11,28] Hu and Bard[11] explained to be due to the repulsive interaction between adsorbed charged thiols.

It is apparent from the time-resolved SEIRA experiment that, during the adsorption of C_{16}TAC, carboxylic acid changes to carboxylate. From this fact, we consider the two-step adsorption mechanism. One is the adsorption of C_{16}TAC and the other is the deprotonation of MPA (Figure 12). Finally, ion pairs of $-COO^{-}\cdot NH_3^{+}-$ connected by the electrostatic interaction are formed.

Conclusions

In situ investigations of SAM formation on gold surface have been carried out by QCM monitor, surface plasmon resonance sensor, and atomic force microscopic techniques.[6−11] In the present work, the surface-enhanced infrared absorption spectroscopy was used for the purpose. It was demonstrated that infrared bands of ATR-SEIRAS are detectable with stronger intensities about 20 times than those of IRAS even for a short alkyl chain compound such as MPA. Moreover, the ATR-SEIRAS was more sensitive than the surface plasmon resonance sensor.[29]

The SAM formation followed the chemical reaction of thiol, the hydrogen-bonding between carboxylic acids, the deprotonation of carboxylic acid, and the rearrangement of adsorbed molecules. The process depended on solvents. Molecular information on the process of the SAM formation is obtained only from IR but not from other techniques described above. The ATR-SEIRAS could also be applied to the adsorption of molecules on the thin films such as C_{16}TAC adsorption on MPA SAM. The kinetics of the SAM formation obeyed the Langmuir theory, consistent with previous reports.[6−8,11] However, this was not a case of the C_{16}TAC adsorption on the MPA SAM.

References and Notes

(1) Dijt, J. C.; Stuart, M. A. C.; Fleer, G. J. *Macromolecules* **1994**, *27*, 3207, 3219, 3229.
(2) Filippova, N. L. *Langmuir* **1998**, *14*, 5929.
(3) Kankare, J.; Vinokurov, I. A. *Langmuir* **1999**, *15*, 591.
(4) Imae, T.; Ito, M.; Aoi, K.; Tsutsumiuchi, K.; Noda, H.; Okada M. *Colloids Surf, A*—Phys. Eng. Asp., in press.
(5) Imae, T.; Ito, M.; Aoi, K.; Tsutsumiuchi, K.; Noda, H.; Okada, M. Submitted.
(6) Shimizu, K.; Yag, I.; Sato, Y.; Uosaki, K. *Langmuir* **1992**, *8*, 1385.
(7) Karpovich, D. S.; Blanchard, G. J. *Langmuir* **1994**, *10*, 3315.
(8) Pan, W.; Durning, C. J.; Turro, N. J. *Langmuir* **1996**, *12*, 4469.
(9) Kim, C. H.; Han, S. W.; Ha, T. H.; Kim, K. *Langmuir* **1999**, *15*, 8399.
(10) Peterlinz, K. A.; Georgiadis, R. *Langmuir* **1996**, *12*, 4731.
(11) Hu, K.; Bard, A. J. *Langmuir* **1998**, *14*, 4790.
(12) Suetaka, W. *Surface Infrared and Raman Spectroscopy: Methods and Application*; Plenum Press: New York, 1995.
(13) Osawa, M. *Bull. Chem. Soc. Jpn.* **1997**, *70*, 2861, and references therein.
(14) Kudelski, A.; Hill, W. *Langmuir* **1999**, *15*, 3162.
(15) Zhang, Z.-J.; Imae, T. Submitted.
(16) Lestelius, M.; Liedberg, B.; Tengvall, P. *Langmuir* **1997**, *13*, 5900.
(17) Tao, Y.-T.; Pandiaraju, S.; Lin, W.-L.; Chen, L.-J. *Langmuir* **1998**, *14*, 145.
(18) Meuse, C. W.; Niaura, G.; Lewis, M. L.; Plant, A. L. *Langmuir* **1998**, *14*, 1604.
(19) Vanderah, D. J.; Meuse, C. W.; Silin, V.; Plant, A. L. *Langmuir* **1998**, *14*, 6916.
(20) Dong, J.; Ozaki, Y.; Nakashima, K. *Macromolecules* **1997**, *30*, 1111.
(21) Jimbo, T.; Tanioka, A.; Minoura, N. *Langmuir* **1999**, *15*, 1829.
(22) Ozaki, Y.; Fujimoto, Y.; Terashita, S.; Katayama, N.; Iriyama, K. *Spectroscopy* **1993**, *8*, 36.
(23) Bertilsson, L.; Potje-Kamloth, K.; Liess H.-D.; Liedberg, B. *Langmuir* **1999**, *15*, 1128.
(24) Fujimoto, Y.; Ozaki, Y.; Kato, T.; Matsumoto, N.; Iriyama, K. *Chem. Phys. Lett.* **1992**, *196*, 347.
(25) Yamamoto, M.; Furuyama, N.; Itoh, K. *J. Phys. Chem.* **1996**, *100*, 18483.
(26) Umemura, J.; Kamata, T.; Kawai, T.; Takenaka, T. *J. Phys. Chem.* **1990**, *94*, 62.
(27) Williams, L. M.; Evans, S. D.; Flynn, T. M.; Marsh, A.; Knowles, P. F.; Bushby, R. J.; Boden, N. *Langmuir* **1997**, *13*, 751.
(28) Bain, C. D.; Troughton, E. B.; Tao, Y.-T.; Evall, J.; Whitesides, G. M.; Nuzzo, R. G. *J. Am. Chem. Soc.* **1989**, *111*, 321.
(29) Ito, M.; Imae, T.; Aoi, K.; Tsutsumiuchi, K.; Noda, H.; Okada, M. Unpublished data.